



# Realization of an SI traceable small force of 10 to 100 micro-Newton using an electrostatic measuring system

Jile Jiang, Gang Hu, Zhimin Zhang

Force and Torque Laboratory, Division of Mechanics and Acoustics, National Institute of Metrology, China

## ABSTRACT

A small force of (10–100)  $\mu\text{N}$  traceable to the International System of Units (SI) has been realized using an electrostatic measuring system at the National Institute of Metrology, China. The key component of the measuring system is a pair of coaxial cylindrical electrodes. The inner electrode is suspended with the support of a self-balanced flexure hinge, while the outer electrode is attached to a piezoelectric moving stage. The stiffness of the self-balanced flexure hinge was also designed so as to be both sufficiently stable and sensitive to the small force applied to the inner electrode. Two sets of cameras were used to capture the shape of the electrodes and to obtain a better coaxial arrangement of the inner and outer electrodes. With the help of a capacitance bridge and a piezoelectric moving stage, the relative standard uncertainty of the capacitance gradient does not exceed 0.04%. Associated with a laser interferometer and a DC voltage power source, the feedback system that controls the position of the inner electrode is responsible for the generation of a force of 10–100  $\mu\text{N}$ . The standard uncertainty associated with the force of 100  $\mu\text{N}$  does not exceed 0.1 %.

Section: RESEARCH PAPER

Keywords: small force; electrostatic; capacitance gradient

Citation: Jile Jiang, Gang Hu, Zhimin Zhang, Realization of an SI traceable small force of 10 to 100 micro-Newton using an electrostatic measuring system, Acta IMEKO, vol. 6, no. 2, article 2, July 2017, identifier: IMEKO-ACTA-06 (2017)-02-02

Section Editor: Min-Seok Kim, Research Institute of Standards and Science, Korea

Received March 18, 2016; In final form February 4, 2017; Published April 2017

Copyright: © 2017 IMEKO. This is an open-access article distributed under the terms of the Creative Commons Attribution 3.0 License, which permits unrestricted use, distribution, and reproduction in any medium, provided the original author and source are credited

Funding: This work was supported by the National Key Technology Research and Development Program of the Ministry of Science and Technology of China, No.2011BAK15B06

Corresponding author: Jile Jiang, e-mail: jiangjl@nim.ac.cn

## 1. INTRODUCTION

The invention of atomic force microscopy (AFM) has had a great impact on the development of nanotechnology [1]. This technology has the capability of characterizing material properties such as the surface morphology and interaction potentials [2], [3]. The reliable measurement of the force based on an AFM tip depends on the accuracy of the spring constant. The determination of the spring constant is essential for the absolute measurement of forces below 1 mN. Many methods have been proposed to estimate the spring constant of the AFM tip, but these methods are not SI traceable and lack accuracy [4]–[9]. High-accuracy measurements of SI traceable small forces in the range 1–100  $\mu\text{N}$  have been realized by several NMIs recently [10]–[15]. Most of the standard devices are based on the electrostatic force, and recently a small force-measuring system based on it has been established. Most parts of the measuring system have been completed and the entire

project will be continued under further arrangement at NIM, China.

## 2. PRINCIPLES

### 2.1. Methodology

A standard measuring system for small forces in the range 10–100  $\mu\text{N}$  has been realized using an electrostatic force. The structure of the entire measuring system is shown schematically in Figure 1. The measuring system was placed in a vacuum chamber and the chamber placed on an optical table supported by six legs. The level of the chamber was adjusted with an air bubble level. The optical table featured a mass block to increase the inertia of the entire system. The inner diameter of the vacuum chamber was 700 mm. Because the vibration from the pump may cause instability of the inner electrode, the measurements were operated under normal air pressure.

The key component of the measuring system is the electrostatic force generator, a pair of coaxial cylindrical electrodes, shown in Figure 1. The inner electrode is mounted on the self-balanced hinge, while the outer electrode is mounted on the moving stage. The self-balanced hinge is made of copper and its spring constant is 11.679 N/m. The inner electrode can be moved along the z axis, nominally parallel to the direction of gravity. The degree of overlap between the two cylinders is measured by a heterodyne laser interferometer.

The surface of the bottom inside the inner electrode is smooth enough to reflect the laser beam. A mirror with an Al and MgS<sub>2</sub> coating was mounted on the outer electrode to reflect the reference laser beam. In order to obtain the proper reflection of the laser beam from two cylinders and a proper coaxial alignment, four main steps were followed. The outer electrode was first adjusted with the air bubble level to ensure that the axial alignment was in the direction of gravity. The laser beam was then tuned to obtain the proper reflection from the outer electrode. The inner electrode was adjusted with the help of an x-y plane moving stage and x-y rotation stages to obtain the desirable alignment to the outer electrode. The alignment is observed by using the shape of the two electrodes. Two cameras were used to capture the shape of the electrodes in the x and y direction. The centric distance of the electrodes should be less than 1 μm and the angle between the axes of the electrodes should be less than 1 mrad. Although a self-balanced hinge is introduced to the system, an unexpected movement of the inner electrode can still be found, as shown in Figure 2. This movement was unpredictable. It measured less than 5 μm in 8 hours when the operators were in the room and less than 1 μm in 80 hours without operators. The creep may have been

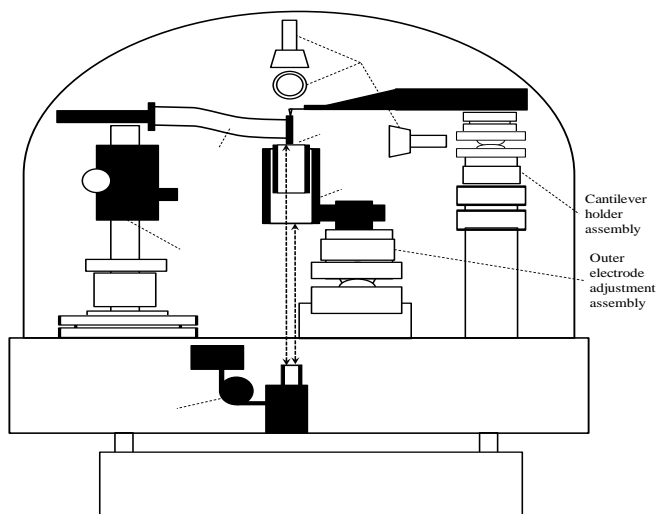


Figure 1. Schematic of the electrostatic measuring system.

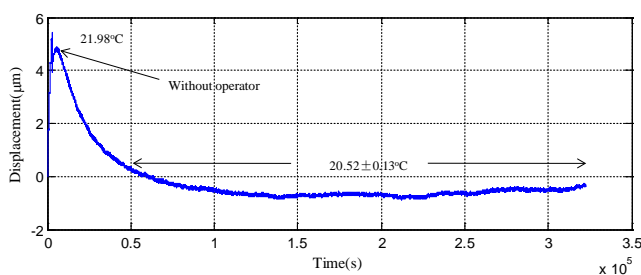


Figure 2. Creep of the inner electrodes.

initiated by temperature variation, because the thermal expansion coefficients of the materials comprising the supporting stages of the inner and outer electrodes are different.

Comparison between the force generated by the coaxial cylinders and a standard weight (1 mg, 2 mg, 5 mg, and 10 mg, provided by Mettler Toledo) was carried out, following the sequence shown in Figure 3. The comparison was achieved by controlling the voltage on the electrodes to maintain a fixed position of the two cylinders. A proportional integral-derivative (PID) method was applied to the system using a computer program. Once the weight was loaded on the inner electrode, the displacement was measured by the interferometer. Then, after the weight was unloaded, an electrostatic force was generated to move the inner electrode to its original position.

## 2.2. Capacitance gradient measurement

The force generated by the system is determined by two factors: the voltage between the two electrodes and the capacitance gradient along the z direction, described as

$$F_e = \frac{1}{2} \frac{dC}{dz} U^2. \quad (1)$$

It is very important to obtain  $dC/dz$  with high accuracy. When measuring the capacitance gradient, the inner electrode is considered to be static. The outer electrode was driven vertically by a piezoelectric stage. The total nominal displacement between the electrodes was 100 μm. In each test,  $dC/dz$  was measured when the displacement between two electrodes was -50, 0, and +50 μm. The outer electrode was held in each position for 30 s. The capacitance was measured by a sensitive bridge (Andeen-Hagerling model AH2700A, Cleveland, OH, USA), while the displacement was measured by the interferometer. Because the reference mirror is fixed to the outer electrode, the displacement from the interferometer equals the displacement between the inner and outer electrode. The creep effect can be disregarded here. As shown in Figure 4,  $dC/dz$  is calculated from the linear fit. Typical measurement results are shown in Figure 4.

As can be seen in the expanded part in Figure 4a, the non-linearity of the capacitance versus displacement in 2 nm may be the cause of the difference and the higher standard deviation.

## 3. COMPARISON TO DEADWEIGHT

The comparisons to deadweights of 1 mg, 2 mg, 5 mg, and 10 mg were carried out after the capacitance gradient was

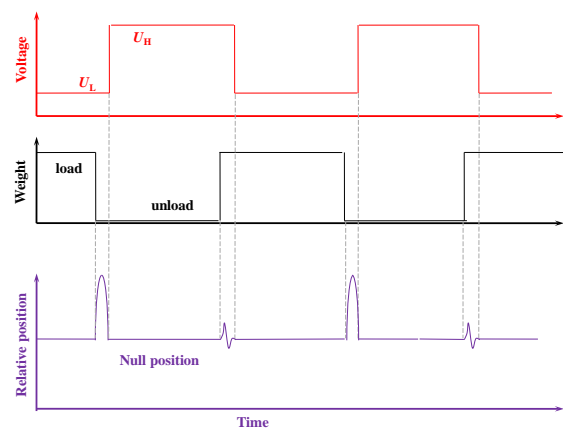


Figure 3. Process of comparison between deadweight and force.

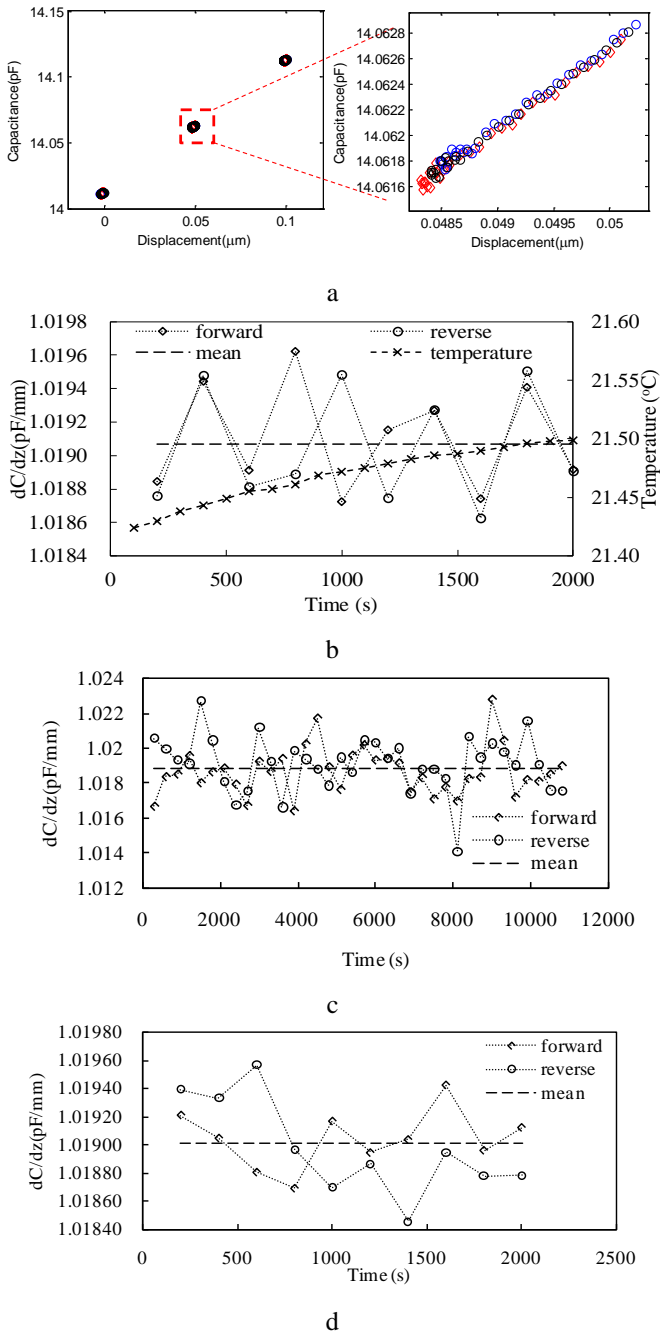


Figure 4. Measurement of the capacitance gradient. a: capacitance values at 0  $\mu\text{m}$  and  $\pm 50 \mu\text{m}$ . Drifts of the capacitance and displacement are 0.0013 pF and 2.5 nm, respectively. b: variation of  $dC/dz$  vs time (mean=1.019077 pF/mm,  $\sigma=3.0 \times 10^{-4}$  pF/mm,  $\sigma/\sqrt{N}=6.7 \times 10^{-5}$  pF/mm). c: capacitance gradient of 35 sets of six points at 0, 10, 20, 30, 40, and 50  $\mu\text{m}$  (mean=1.018901 pF/mm,  $\sigma=1.5 \times 10^{-3}$  pF/mm,  $\sigma/\sqrt{N}=1.8 \times 10^{-4}$  pF/mm),  $21.75 \pm 0.12 \text{ }^\circ\text{C}$ . d: capacitance gradient of 10 sets of nine points at 0, 12.5, 25, 37.5, 50, 62.5, 75, 87.5, and 100  $\mu\text{m}$  (mean=1.019012 pF/mm,  $\sigma=3 \times 10^{-4}$  pF/mm,  $\sigma/\sqrt{N}=6.2 \times 10^{-5}$  pF/mm),  $21.54 \pm 0.11 \text{ }^\circ\text{C}$ .

measured. The comparison procedure is shown in Figure 3. The voltage was held for approximately 200 s once the deadweight was loaded and unloaded. Data acquisition was applied all the time, but after 100 s the value of the voltage can be considered stable. Nominally, the room temperature was  $21.0 \pm 0.5 \text{ }^\circ\text{C}$ . The typical response of the voltage and displacement of the inner electrode is shown in Figure 5, in which the deadweight artefact was 10 mg. Comparison between

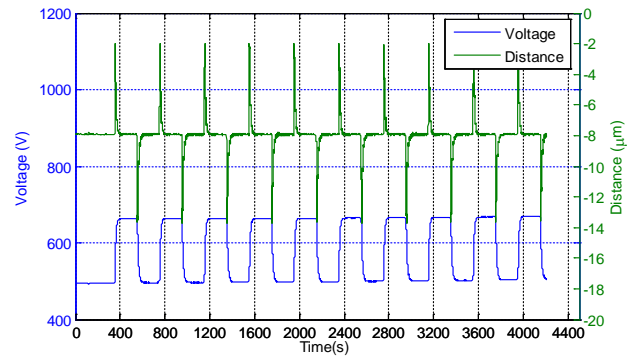


Figure 5. Variations of the voltage and displacement of the inner electrodes when a deadweight of 10 mg was applied.

deadweights of 1 mg, 2 mg, 5 mg, and 10 mg is shown in Table 1. The relative standard deviation of the electrostatic force  $F_e$  became smaller when the larger deadweight was loaded.

#### 4. UNCERTAINTY

Considering (1) and assuming all the factors are uncorrelated, the uncertainty of the measuring force is

$$u^2(f) = \left( \frac{\partial f}{\partial (dC)} \right)^2 u^2 \left( \frac{dC}{dz} \right) + \left( \frac{\partial f}{\partial (U)} \right)^2 u^2(U), \quad (2)$$

where the capacitance gradient is obtained by the following method:

$$\frac{dC}{dz} = \frac{\sum_{i=1}^n (z_i - \bar{z})(c_i - \bar{c})}{\sum_{i=1}^n (z_i - \bar{z})^2}. \quad (3)$$

$c_i$  is the capacitance value corresponding to the relative displacement of the inner electrode,  $z_i$ . The average values of  $c_i$  and  $z_i$  are  $\bar{c}$  and  $\bar{z}$ , respectively. It can be verified that

$$\frac{\partial dC}{\partial z_i} dz_i = \left( \frac{c_i}{\sum_{i=1}^n z_i^2} - \frac{2 \sum_{i=1}^n c_i z_i}{\left( \sum_{i=1}^n z_i^2 \right)^2} z_i - \frac{\bar{c}}{\sum_{i=1}^n z_i^2} + \frac{\bar{c} \sum_{i=1}^n z_i}{\left( \sum_{i=1}^n z_i^2 \right)^2} 2z_i \right) dz_i \quad (4)$$

and

$$\frac{\partial dC}{\partial C_i} dC_i = \frac{z_i}{\sum_{i=1}^n z_i^2} dC_i. \quad (5)$$

The uncertainty associated from a linear fit by the least square method, to determine the capacitance gradient, can be omitted.

The relative standard uncertainty of the force generated by the system is expressed as

$$\frac{u(f)}{f} = \sqrt{u_r(r)^2 + u_r(C)^2 + u_r(z)^2 + u_r(d)^2 + 4u_r(U)^2}. \quad (6)$$

$u_r(r)$  is caused mainly by the repeatability of  $dC/dz$ , associated with vibrations from the air flow and the unexpected vibration from the base. The actual displacements of the inner and outer electrodes were measured by the laser interferometer, so  $u_r(z)$  should be considered.  $u_r(U)$  is caused by voltage noise from the

Table 1. Comparison between deadweights of 1, 2, 5, and 10 mg.

Gravity of deadweight $G$ ( $\mu\text{N}$ , with expanded uncertainty, $k=2$ )	Electrostatic force $F_e$ ( $\mu\text{N}$ )	Relative standard deviation of $F_e$ , $\sigma$	$(F_e - G)/G$ (%)
9.806±0.002	9.8008	0.0112	-0.055
19.609±0.002	19.595	0.0143	-0.071
49.009±0.002	48.746	0.0025	-0.54
98.021±0.002	97.455	0.00074	-0.58

DC power source. This is related to the actual force generated. Noise in the measurement of the capacitance,  $u_r(C)$ , and the displacement error of the piezoelectric moving stage,  $u_r(d)$ , are also included.

According to the calibration results of the AH2700A capacitance bridge, the DC power source, the laser interferometer, and the piezoelectric stage, the relative standard uncertainties  $u_r(C)$ ,  $u_r(U)$ ,  $u_r(z)$ , and  $u_r(d)$  are  $0.5 \times 10^{-6}$ ,  $2.5 \times 10^{-5}$ ,  $1 \times 10^{-8}$ , and  $1 \times 10^{-4}$ , respectively. According to the results shown in Figure 4,  $u(r) = 1.8 \times 10^{-4}$  pF/mm, and the relative standard uncertainty of the force generated by the system is  $2.69 \times 10^{-4}$ .

According to the results of the comparison shown in Table 1, the relative difference between the electrostatic force and the gravity of the deadweight is larger than  $2.69 \times 10^{-4}$ . In general, the following aspects should be considered: 1) The test mass is placed close to the inner electrode. The shapes of these test masses are different, which will affect the actual capacitance measurement since the mass is lifted by the stainless-steel wire and attached directly to the self-balanced hinge. 2) The fork used to lift the test mass is made of stainless steel and is isolated from the ground. Considering that the outer electrode is grounded and the inner electrode is applied to a high voltage, the test mass can be electrically charged and attracted by the inner electrode. This could be studied by reversing the polarity of the electrodes. The possible primary improvement of the system should be realized by electrically isolating the inner and outer electrodes from the other parts, especially the test mass.

## 5. CONCLUSIONS

Forces of (10–100)  $\mu\text{N}$  traceable to the International System of Units (SI) were realized by a measuring system based on electrostatic force. Primary analysis shows a relative standard uncertainty of  $2.69 \times 10^{-4}$ . The deviation between deadweight and the electrostatic force was less than 0.6 %.

## ACKNOWLEDGEMENTS

This study was supported by “Research on measurement standards and reference materials based on micro-nano technology” (No. 2011BAK15B00) and by “Research on key technologies in establishment and traceability of microgram mass standards and micro-nano force standards” (No. 2011BAK15B06), both subprojects of the National Key Technology Research and Development Program of the Ministry of Science and Technology of China.

## REFERENCES

- [1] Binning G, Quate C F, Gerber Ch, “Atomic Force Microscope”, *Phys. Rev. Lett.*, 56(1986) pp. 930-933.
- [2] Baibich M N, Broto J M, Fert A,” Giant Magnetoresistance of (001) Fe/(001)Cr Magnetic Superlattices”, *Phy. Rev. Lett.*, 61(1988) pp. 2472-2475.
- [3] Wu S, Fu X, Hu X D, “Manipulation and behavior modeling of one-dimensional nanomaterials on a structured surface”. *Appl. Surf. Sci.*, 256(2010) pp. 4738-4744.
- [4] Clifford C A, Seah M P, “The determination of atomic force microscope cantilever spring constants via dimensional methods for nanomechanical analysis” . *Nanotechnology*, 16(2005) pp. 1666-1680.
- [5] Neumeister J M, Ducker W A. “Lateral normal and longitudinal spring constants of atomic force microscopy cantilevers” . *Rev. Sci. Instrum.*, 65(1994) pp. 2527-2531.
- [6] Cleveland J P, Manne S, Bocek D, et al. “A Nondestructive Method for Determining the Spring Constant of Cantilevers for Scanning Force Microscopy” . *Rev. Sci. Instrum.*, 64(1993) pp. 403-405.
- [7] Burnham N A, Chen X, Hodges C S et al., “Comparison of calibration methods for atomic-force microscopy cantilevers”, *Nanotechnology*, 14(2003) pp. 1-6.
- [8] Sader J E, Chon JWM, Mulvaney P. “Calibration of rectangular atomic force microscope cantilevers”. *Rev. Sci. Instrum.*, 70(1995) pp. 3967-3969.
- [9] Ohler B. “Cantilever spring constant calibration using laser Doppler vibrometry” . *Rev. Sci. Instrum.*, 78(2007) pp. 063701-063701-5.
- [10] Pratt J R, Newell D B, Kramar J A. “A flexure balance with adjustable restoring torque for nanonewton force measurement. Joint International Conference IMEKO TC3/TC5/TC20, Celle, GE: VDI BERICHTE, 2002, 1685 pp. 77-822
- [11] Pratt J R, Smith D T, Kramar J A, “Microforce and Instrumented Indentation Research at the National Institute of Standards and Technology, Gaithersburg, MD[R]: Charlotte, NC: NIST, 2003.
- [12] Christopher W J, Richard K L. “Review of Low Force Transfer Artefact Technologies, Report ENG 5 [R]. Middlesex: NPL, 2008.
- [13] Richard K L, Simon O. 2004. “Design of a bi-directional electrostatic actuator for realising nanonewton to micronewton forces, Report DEPC-EM 001[R]. Middlesex: NPL, 2004.
- [14] Chen SJ, Pan S S. “A force measurement system based on an electrostatic sensing and actuating technique for calibrating force in a micronewton range with a resolution of nanonewton scale” . *Meas. Sci. Technol.*, 22(2011) pp 045104-045104-8.
- [15] Vladimir N. “Facility and methods for the measurement of micro and nano forces in the range below 10<sup>-5</sup> N with a resolution of 10-12N (development concept)”. *Meas. Sci. Technol.*, 2007, 18(2007) pp. 360-366.